Journal of Hydrology 656 (2025) 133014

Contents lists available at ScienceDirect

Journal of Hydrology

journal homepage: www.elsevier.com/locate/jhydrol

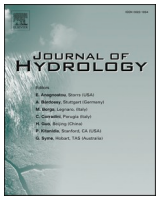

Research papers

A criterion to reduce chamber method uncertainty when measuring plant transpired vapor isotopes

Yusen Yuan [a,b,*], Manoj K. Shukla [a,c], Kenneth C. Carroll [a], Lixin Wang [d], Hui Yang [a,b], Taisheng Du [b]

[a] Department of Plant and Environmental Sciences, New Mexico State University, Las Cruces 88003, USA
[b] Center for Agricultural Water Research in China, China Agricultural University, Beijing 100083, China
[c] Department of Crop and Soil Science, Oregon State University, Corvallis, OR 97331, USA
[d] Department of Earth and Environmental Sciences, Indiana University Indianapolis, Indianapolis, IN 46202, USA

ARTICLE INFO

This manuscript was handled by Huaming Guo, Editor-in-Chief, with the assistance of Tomoko Ohta, Associate Editor.

Keywords:
Isotopes
Plant Transpiration
Chamber Method
Evapotranspiration
Maize

ABSTRACT

The isotopic composition of plant transpiration (δ_T) is an important parameter to understand the change of water phase at the transpired site and isotope-based evapotranspiration partitioning. The isotope-steady-state (ISS) method and the chamber method are two common methods to measure and simulate δ_T. The ISS method can only be used within a short period of a day and has been challenged due to biases in cryogenic extractions, whereas the representativeness of a leaf level δ_T based on the chamber method has also been considered questionable. In this study, we examined the heterogeneity in the leaf level chamber method, as well as estimating the whole plant δ_T based on both the ISS method and the chamber method at a maize field. Results showed that the ^{18}O and ^{2}H results of the ISS method and the chamber method were strongly correlated, which supported the validity of cryogenic extraction-associated methodology in maize stems. The accuracy of the chamber method and the precision of the chamber method were positively correlated. This study proposed a new diagnostic factor (C_m/C_v) that negatively affected the uncertainty of the leaf and plant chamber method, and supported a dynamic uncertainty rather than an assumed constant chamber method uncertainty value. The chamber method uncertainty would always be greater than the isotope analyzer system error, whereas the increase of plant transpiration and/or the decrease of background vapor concertation will decrease the chamber method uncertainty. More rigorous uncertainty checks should be considered when using chamber method to measure the isotope composition of soil evaporation due to generally less vapor flux than that of plant transpiration. We suggest a three-step criterion to quantitatively evaluate the chamber method and ensure data quality: 1). Use C_m/C_v values of several test measurements to approximate whether the chamber method is suitable at the location; 2). Results should not be considered when water condensation occurs; and 3). Present chamber uncertainty together with δ_T calculation.

1. Introduction

Plant transpiration (T) is generally considered to be at least 65 % of terrestrial evapotranspiration (ET) (Wang et al., 2014), and has a strong influence on the terrestrial water cycle (Wang and Dickinson, 2012). Stable isotopes of hydrogen and oxygen (^{2}H and ^{18}O) are powerful tracers to detect these effects. As a source tracer, the isotopic composition of plant transpiration (δ_T) dominates the variability of the isotopic composition of ET (Yuan et al., 2022; Yuan et al., 2024) and atmospheric vapor (Farquhar et al., 2007). As a sink tracer, δ_T is related to the isotopic composition of the liquid water at the transpired site (δ_{LT}) (Welp et al., 2008; Cernusak et al., 2022). As one of the three input parameters in isotope-based ET partitioning (Xiao et al., 2018; Rothfuss et al., 2021), only a few methods could measure or estimate δ_T (Wang et al., 2012) compared with that of the isotopic composition of E (δ_E) (Craig and Gordon, 1965) and the isotopic composition of ET (δ_{ET}) (Keeling, 1958; Yakir and Sternberg, 2000). Interestingly, about 22 % of the variations of T/ET is induced by the change in δ_T (Cui et al., 2020; Yuan et al., 2022). Thus, the accurate and precise estimates of δ_T are of great importance.

The water in the stem or xylem of the plant was originally used to represent the transpiration water, and it was assumed to be equal to the

* Corresponding author.
E-mail address: yuseny@nmsu.edu (Y. Yuan).

https://doi.org/10.1016/j.jhydrol.2025.133014
Received 7 August 2024; Received in revised form 5 February 2025; Accepted 21 February 2025
Available online 5 March 2025

isotopic composition of the water absorbed by the root system. This assumption is valid when plant is under the isotope-steady-state (ISS) condition (Flanagan et al., 1991; Zhang et al., 2011; Zhao et al., 2016). The ISS condition is only met during a very short period at noon time (Lee et al., 2007; Welp et al., 2008; Peters and Yakir, 2010), when transpiration rates of plants are high and vapor pressure deficit of atmosphere is relative stable (Harwood et al., 1998). This assumption is usually not satisfied in daily and long-term time series when non-steady-state (NSS) conditions dominate, which is caused by changes in relative humidity and leaf energy balance (Farquhar and Cernusak, 2005; Lai et al., 2008). To circumvent NSS transpiration limitations, some researchers have proposed that the transpiration characteristics of the typical bulk leaf can be used to represent the transpiration characteristics of the entire plant, as δ_{LT} can be quantified by a modified model (Dongmann et al., 1974; Farquhar and Cernusak, 2005) based on Craig-Gordon model (Craig and Gordon, 1965). However, this sort of substitution has multiple challenges. For example, the isotopic composition within one leaf is heterogenous (Gan et al., 2002) because of the Péclet effect (Farquhar and Lloyd, 1993), resulting in uncertainty in selecting a representative transpired site when using the modified Craig-Gordon model. As another illustration, even if the modified Craig-Gordon model at leaf scale is reliable, it is also difficult to upscale from one leaf to the whole plant, as the isotopic composition of different leaves are heterogeneous (Wu, 2017). The necessity of NSS conditions at the leaf level is challenged, as its performance in the Iso-SPAC model (coupled heat, water, and isotopic tracer in the soil–plant-atmosphere continuum) is not significantly better than the ISS assumption (Wang et al., 2015; Wang et al., 2018). Furthermore, whether or not the cryogenic extracted xylem water could represent the transpired water during the ISS has been challenged in recent years (Chen et al., 2020). These potential factors may cause large errors and uncertainties in the subsequent calculations relying on δ_T (Roden and Ehleringer, 1999).

In the recent decade, a chamber method based on basic gas exchange principles to directly measure δ_{LT} has been developed (Wang et al., 2012; Dubbert et al., 2013), which benefits from the widely-used, high-frequency laser spectroscopy (Kerstel and Gianfrani, 2008; Wang et al., 2009). The advantages of the chamber are obtaining δ_{LT} without using complex isotope models, enabling the measurement of integrated fluxes from different leaves, and allowing for continuous monitoring of gas exchange and isotopic composition over time (Zuecco et al., 2022). The chamber method has been successfully applied on forest ecosystems (Lanning et al., 2020), farmland ecosystems (Lu et al., 2017), and grassland ecosystems (Cui et al., 2020). However, it has been rarely applied to the entire plant scale δ_T (Wu, 2017; Tian et al., 2020), and its accuracy, precision, and uncertainty still need to be evaluated.

Herein, we estimated the whole plant δ_T based on the ISS method and the chamber method on a maize field. Due to the restrictions of ISS condition, we applied the two methods at 11:00 am and 1:00 pm on 36 sunny days in 2017. The accuracy, precision, and uncertainty of the chamber method are presented. The leaf level chamber was conducted on July 17, 2017 to verify the requirement of whole plant level chamber method. The purpose of this study is to provide an important reference for the leaf chamber method to quantify the δ_T of the whole plant, to reveal the main factors affecting the chamber method uncertainty, and to suggest a criterion to increase chamber method accuracy while reducing its uncertainty.

2. Materials and methods

2.1. Site Description

The experiment was conducted in an arid area of northwestern China during the spring maize growing season in 2017 within the Shiyang River Basin (37°52′ N, 102°50′ E, 1581 m). The average temperature at this location is 8 °C, the annual accumulated temperature is 3550 °C, and the average annual sunshine duration is 3000 h and the frost-free period is 150 days. The annual precipitation is 164 mm, but the annual pan evaporation is greater than 2000 mm. The groundwater depth is 40–50 m. The soil texture at 0–0.8 m deep is silty loam, the average soil dry bulk density is 1.52 g cm^{-3}, and the average field capacity is 0.29 m^3 m^{-3}. Maize was planted with row spacing of 40 cm and plant spacing of 30 cm. The plant density was about 66,000 plants per hectare and the total area was about 39 ha. Crops were sowed on April 20 and harvested on September 15.

2.2. Experiment design

The samples collected during the experiment were plant xylem samples, mixed water vapor in plant chamber, mixed water vapor in leaf chamber, and atmospheric water vapor. The specific collection method was as follows. When collecting xylem samples, the chlorophyll-free part of stem below the ground surface was selected to avoid the effect of isotope fractionation caused by plant transpiration. The xylem samples were obtained after removing the phloem from the stem. The xylem samples were collected at 11:00 am and 1:00 pm on sunny days and were sealed in ziplock bags for temporary storage. A plant soil water vacuum extraction system (LI-2000, LICA United Technology, China) was used to obtain plant xylem liquid water, and the extraction method followed methods described by Orlowski et al. (2013). The extracted xylem liquid water samples were measured using an isotope analyzer (Picarro L2130-i, Picarro, USA) when conducting liquid water measurement mode. The liquid water isotope value calibration process was the same as that of Zhao et al. (2019).

Vapor samples, including mixed water vapor in plant chamber, mixed water vapor in leaf chamber, and atmospheric water vapor, were measured by the same *in-situ* isotope analyzer when running water vapor measurement mode. The date and time of measurement are shown in Supplementary. The schematic of the chamber system was shown in Fig. 1. The atmospheric water vapor was collected by gas trap #1 of the system, which is from canopy height. The canopy height trap was

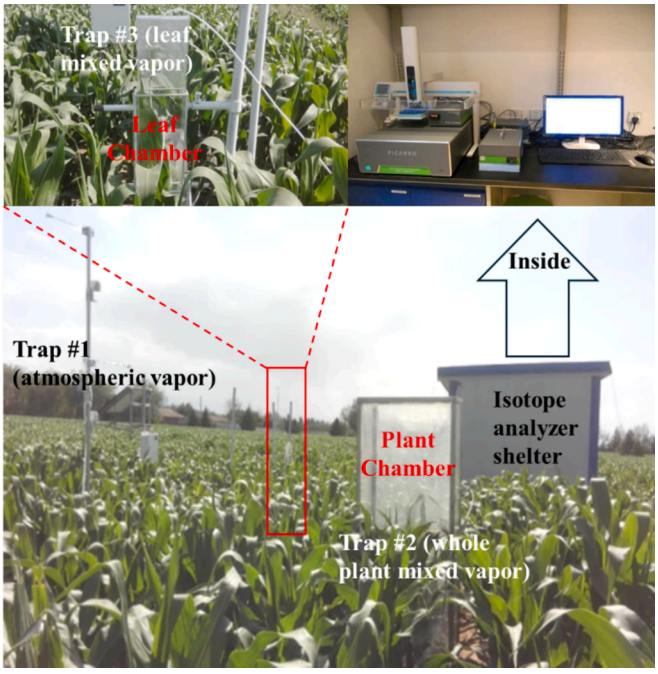

Fig. 1. Schematic of the transpiration chamber system. The system is made up of the atmosphere vapor suction port (trap #1), an acrylic plant chamber with volumes of 40 x 60 x 180 cm (connected with isotope analyzer by trap #2), an acrylic leaf chamber with volumes of 10 x 20 x 80 cm (connected with isotope analyzer by trap #3), and Teflon tube which connects to the suction port or the chamber with water vapor isotope analyzer.

adjusted with the growth of corn, and generally did not exceed 1.8 m. The mixed vapor from the plant chamber was collected through gas trap #2, and the mixed vapor from the leaf chamber was collected through gas trap #3. Teflon tubes were used to connect traps and the isotope analyzer. The vacuum flow rate in the Teflon tube is 1,000 cm^3 min^{-1}.

Gas trap #2 connected with a size of 40 cm x 60 cm 180 cm transparent acrylic chamber, and the sampling time of the mixed vapor from plant chamber was the same as the time for taking the plant xylem water sample. Two holes with a diameter of 6 mm opened on both sides of 40 cm x 180 cm. One hole was for connecting the chamber with the isotope analyzer, and the other hole directly connected to the free atmosphere. To thorough mix the vapor from transpired source and atmospheric source, a fan was embedded inside the chamber, which followed methods presented in Song et al. (2015). The structure of the chamber system was same as the design used in our prior work (Yuan et al., 2022), whereas the chamber was expanded to cover the whole plant. The theoretical basis of this design is mainly derived from the principle of gas exchange (Zhao et al., 2019).

Gas trap #3 connected with a size of 10 cm x 20 cm x 80 cm transparent acrylic chamber to fit the leaves shape. A tripod was used to adjust the chamber to fit a single plant leaf. The leaf chamber samples were measured nine times on July 17 at around 11:15 am just after the measurement of plant chamber samples. An upper leaf, a middle leaf, and a bottom leaf were measured three times each.

Each gas trap was conducted for a total of 225 s. As the analyzer makes a measurement every 0.9–1 s, approximately 259–264 values for each trap were recorded. For each 225 s measurement period, No. 195 to No. 253 data points were used to avoid memory issues and influence of transient pressure variation. The isotope analyzer output the atmospheric vapor concentration (C_v) and isotopic composition of atmospheric vapor (δ_v) results from gas trap #1, and output the mix vapor concentration (C_m) and isotopic composition of mix vapor (δ_m) results from gas trap #2 and #3. δ_v values included the ^{18}O isotope composition of atmospheric vapor ($\delta^{18}O_v$), and the ^{2}H isotope composition of atmospheric vapor ($\delta^{2}H_v$). δ_m values included the ^{18}O isotope composition of the mix vapor ($\delta^{18}O_m$), and the ^{2}H isotope composition of the mix vapor ($\delta^{2}H_m$). Vapor specifications ensure the precision of a measurement ranging from 1,000 to 50,000 ppm, the precision is ± 0.2 ‰ for $\delta^{18}O$ and ± 1.0 ‰ for $\delta^{2}H$ (Zhao et al., 2019). Our vapor calibration followed Yuan et al. (2020). To minimize the influence of isotopic concentration dependence, measured δ_v and δ_m were calibrated. C_v and C_m were used directly as their actual values. The C_v and C_m in the chamber measurement ranged from 11,064 ppm to 38,580 ppm. Thus, gradients of 10,000 ~ 20,000 ppm, 20,000 ~ 30,000 ppm, and 30,000 ~ 40,000 ppm were selected as calibration concentrations. The Vienna Standard Mean Ocean Water kit was measured at 15,000 ppm, 25,000 ppm, and 35,000 ppm, to improve the precision of δ_v and δ_m at the range of 10,000 ~ 20,000 ppm, 20,000 ~ 30,000 ppm, and 30,000 ~ 40,000 ppm, respectively.

2.3. Obtaining δ_T using the isotope Steady-State assumption method

The isotope composition of the xylem water (δ_x) is assumed to be under the ISS condition and represent whole plant δ_T (δ_{Tx}) during the noon time when transpired rate was the highest during the day. The change in plant water storage during this period is considered to be zero. In this study, we also assumed that δ_{Tx} is a true value of δ_T to evaluate the performances of the chamber method.

2.4. Obtaining δ_T using the chamber method

Following the basic gas exchange principle (Von Caemmerer and Farquhar, 1981), the chamber method measures δ_T directly as follows (Wang et al., 2012) when assuming transpiration rate is constant during the measurement:

$$\delta^{18}O_{Tc} = \frac{C_m\delta^{18}O_m - C_v\delta^{18}O_v}{C_m - C_v} \quad (1)$$

$$\delta^{2}H_{Tc} = \frac{C_m\delta^{2}H_m - C_v\delta^{2}H_v}{C_m - C_v} \quad (2)$$

where δ_{Tc} represents the plant transpiration measured using the chamber method attributed to whole plant level δ_T. The leaf level δ_T values (δ_{LTc}) are calculated in a similar way.

2.5. Monitoring potential condensation in the chamber

The reliability of the chamber method was mainly challenged, because it does not account for condensed water in the chamber. The condensed water in the chamber likely influences the precision and accuracy of the chamber method. To access the vapor conditions in the chamber, we calculated the actual vapor pressure (e_a, kPa) and the saturated vapor pressure (e_s, kPa) (Tetens, 1930) in the chamber by:

$$e_a = C_v{*}M(H_2O){*}p{*}10^{-6} \quad (3)$$

$$e_s = 0.611{*}\exp(17.27{*}T_c/(T_c + 273)) \quad (4)$$

where $M(H_2O)$ is the molecular weight of water ($18.02{*}10^{-3}$ kg/mol). p is the local air pressure, which is approximately 0.85 x 10^3 kPa. T_C in ℃ is the temperature in the chamber. Here we use e_a and e_s as quality controllers to detect the vapor situations in the chamber. If $e_a < e_s$, there is no condensed water inside the chamber; if $e_a \geq e_s$, condensation might occur in the chamber.

2.6. Using the concordance correlation coefficient (ρ_c) to access precision and accuracy

The ρ_c calculated to account for repeated measures is used to determine both precision and accuracy by determining the deviation of the data from the best-fit linear line. The formula was proposed by Lawrence and Lin (1992), and was shown as follows:

$$\rho_c = \rho_r C_b \quad (5)$$

where ρ_r is correlation coefficient of linear regression line, which reflected the system error as well as the precision of a model. C_b is a parameter to quantify the distance the best-fit line deviates from the 1:1 concordance line, which reflects the accuracy of a model:

$$C_b = \frac{2\sigma_x\sigma_y}{\sigma_x^2 + \sigma_y^2 + (\mu_x - \mu_y)^2} \quad (6)$$

where μ_x and μ_y represent the mean value of simulated results and the mean value of measured results, respectively. σ_x and σ_y represent the standard deviation of simulated results and the standard deviation of measured results, respectively. The range of ρ_r and C_b is (0, 1]. The larger value of ρ_r or C_b means more precise or accurate of the model (Nilsson et al., 2010).

2.7. Uncertainty of the chamber method

The δ_{Tc} uncertainty analysis was expressed as the first-order Taylor series approximation (Phillips and Gregg, 2001) when assuming δ_m, δ_v, C_m, and C_v were independent:

$$\sigma^2(\delta_{Tc}) = \frac{\partial^2(\delta_{Tc})}{\partial^2(\delta_m)}\sigma^2(\delta_m) + \frac{\partial^2(\delta_{Tc})}{\partial^2(\delta_v)}\sigma^2(\delta_v) + \frac{\partial^2(\delta_{Tc})}{\partial^2(C_m)}\sigma^2(C_m) + \frac{\partial^2(\delta_{Tc})}{\partial^2(C_v)}\sigma^2(C_v) \quad (7)$$

where $\sigma(\delta_{Tc})$, $\sigma(\delta_m)$, $\sigma(\delta_v)$, $\sigma(C_m)$, and $\sigma(C_v)$ represent the uncertainty of δ_{Tc}, δ_m, δ_v, C_m, and C_v, respectively. Thus, $\sigma(\delta_{Tc})$ is the combination of

the uncertainty from the isotope values ($\sigma(\sum\delta)$) and the uncertainty from the vapor concentration ($\sigma(\sum C)$):

$$\sigma^2(\delta_{Tc}) = \sigma^2(\sum\delta) + \sigma^2(\sum C) \quad (8)$$

where

$$\sigma^2(\sum\delta) = \frac{\partial^2(\delta_{Tc})}{\partial^2(\delta_m)}\sigma^2(\delta_m) + \frac{\partial^2(\delta_{Tc})}{\partial^2(\delta_v)}\sigma^2(\delta_v) = \left(\frac{C_m}{C_m - C_v}\right)^2\sigma^2(\delta_m) + \left(\frac{C_v}{C_m - C_v}\right)^2\sigma^2(\delta_v)$$

and $\sigma^2(\sum C) = \frac{\partial^2(\delta_{Tc})}{\partial^2(C_m)}\sigma^2(C_m) + \frac{\partial^2(\delta_{Tc})}{\partial^2(C_v)}\sigma^2(C_v) = \left(\frac{C_v(\delta_m - \delta_v)}{(C_m - C_v)^2}\right)^2\sigma^2(C_m) + \left(\frac{C_m(\delta_m - \delta_v)}{(C_m - C_v)^2}\right)^2\sigma^2(C_v)$. Similarly, the uncertainty of δ_{LTc} ($\sigma(\delta_{LTc})$) was calculated in terms of Eq. (7).

3. Results

3.1. The relationship between δ_{Tx} and δ_{Tc}

The δ_{Tx} and δ_{Tc} values among overall 72 observation points are shown in Appendix A. Supplementary data. We removed 19 observation points where $e_a \geq e_s$, because they indicated potential condensation. The average $\delta^{18}O_{Tc}$ and δ^2H_{Tc} values (after the quality control filter and potential condensation impacted data removal) were −9.49 ‰ ± 2.21 ‰ and −72.65 ‰ ± 13.47 ‰, respectively. The average $\delta^{18}O_{Tx}$ and δ^2H_{Tx} values were −9.27 ‰ ± 2.07 ‰ and −71.99 ‰ ± 12.80 ‰, respectively. The linear regressions between δ_{Tx} and δ_{Tc}, for both ^{18}O and ^2H, were highly significant ($\delta^{18}O_{Tc} = 0.97\ \delta^{18}O_{Tx} - 0.48$ ‰, $r^2 = 0.83^{***}$, n = 53; $\delta^2H_{Tc} = 0.99\ \delta^2H_{Tx} - 0.99$ ‰, $r^2 = 0.90^{***}$, n = 53) as was shown on Fig. 2 **(a)** and **(b)**. The ρ_r, C_b, and ρ_c values of the chamber method in ^2H were slightly greater than that of the chamber method in ^{18}O, which were both more than 0.90.

As for the results of different months (Table 1, except July due to lack of data after the condensation filter), the linear regression between δ_{Tx} and δ_{Tc} results (both ^{18}O and ^2H) were highly significant ($p < 0.01$) in September and were highly significant ($p < 0.001$) in May, June, and August. The ranking for r^2, ρ_r, C_b, and ρ_c values of the regressions were August > June > September > May. The r^2, ρ_r, C_b, and ρ_c values of ^2H regressions were greater than the corresponding r^2 values of ^{18}O regression.

3.2. The uncertainty of δ_{Tc}

$\sigma(\delta_{Tc})$ was calculated from Eq. (7), which included the uncertainty parameters of $\sigma(\delta_m)$, $\sigma(\delta_v)$, $\sigma(C_m)$, and $\sigma(C_v)$. The average $\sigma(\delta_m)$ and $\sigma(\delta_v)$ for ^{18}O was 0.20 ‰ and 0.21 ‰, respectively. The average $\sigma(\delta_m)$ and $\sigma(\delta_v)$ for ^2H was 1.02 ‰ and 1.00 ‰, respectively. The average $\sigma(C_m)$ and $\sigma(C_v)$ was 100.10 ppm and 113.56 ppm.

Among the 53 observation points after the filtering, the average $\sigma(\delta_{Tc})$ of ^2H was ± 8.45 ‰, which was 4.91 times larger than the average $\sigma(\delta_{Tc})$ of ^{18}O (± 1.72 ‰). The average $\sigma(\delta_{Tc})$ of ^2H in May, June, July, August, and September was ± 9.89 ‰, ± 7.50 ‰, ± 7.99 ‰, ± 8.03 ‰, and ± 9.29 ‰, respectively. The average $\sigma(\delta_{Tc})$ of ^{18}O in May, June, July, August, and September was ± 2.10 ‰, ± 1.51 ‰, ± 1.53 ‰, ± 1.62 ‰, and ± 1.78 ‰, respectively. In ^2H of $\sigma(\delta_{Tc})$, the δ_{Tc} uncertainty from the measured isotope values (± 8.43 ‰) was 14.53 times of the uncertainty from the measured vapor concentration (± 0.58 ‰). In ^{18}O of $\sigma(\delta_{Tc})$, the δ_{Tc} uncertainty from the measured isotope values (± 1.71 ‰) was 7.75 times larger than the uncertainty from the measured vapor concentration (± 0.22 ‰).

The square of $\sigma(\delta_{Tc})$ was negatively correlated to C_m/C_v for both ^2H and ^{18}O (Fig. 3). The quantitative relationship between the square of $\sigma(\delta_{Tc})$ and C_m/C_v will be specified in section 4.2. Among the 53 observation points after the filter, the average C_m/C_v was 1.19. The average C_m/C_v in May, June, July, August, and September was 1.15, 1.20, 1.22, 1.18, and 1.19, respectively.

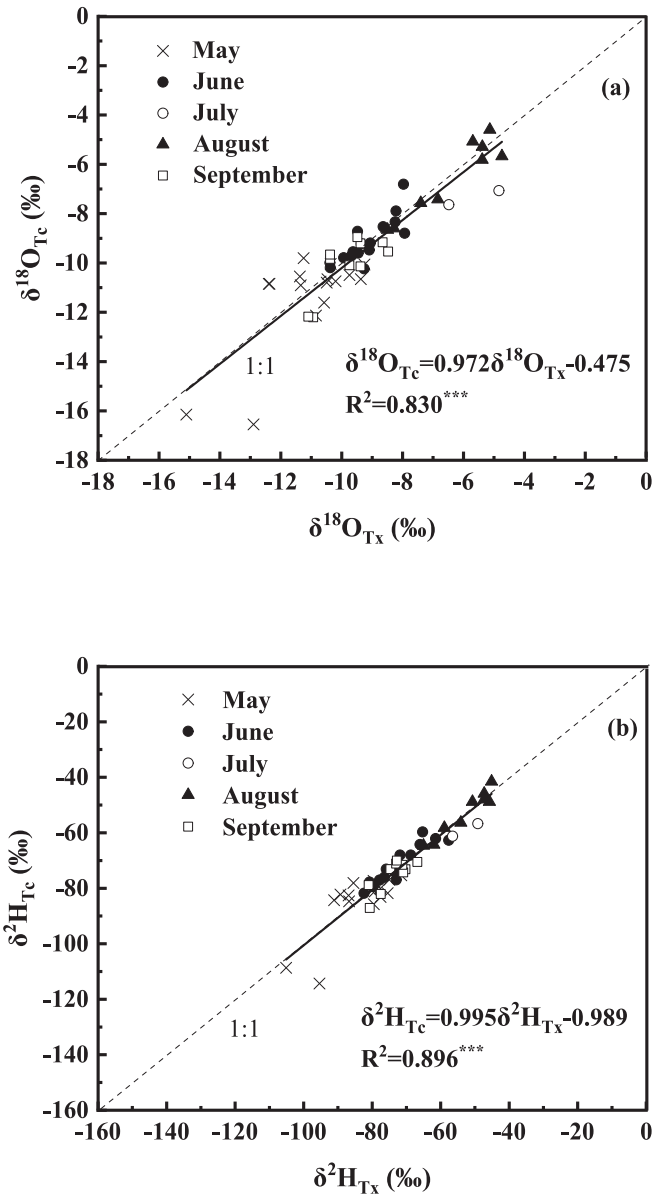

Fig. 2. The linear regressions between δ_{Tx} and δ_{Tc} (n = 53) among different months after the water condensation filter for (a) ^{18}O and (b) ^2H.

3.3. Leaf level chamber method

The δ_{LTc} values among the three leaves on July 17 are presented in Table 2. All of the δ_{LTc} met the filter that $e_a < e_s$, which ensured that no δ_{LTc} value was removed. The average $\delta^{18}O_{LTc}$ from the upper leaf, the middle leaf, and the lower leaf were −5.83 ‰, −12.84 ‰, and −13.25 ‰, respectively. The average δ^2H_{LTc} from the upper leaf, the middle leaf, and the lower leaf were −51.65 ‰, −99.29 ‰, and −82.62 ‰, respectively. The average $\delta^{18}O_{LTc}$ and δ^2H_{LTc} among all nine measurements were −10.64 ‰ and −77.58 ‰, respectively. The standard deviations of $\delta^{18}O_{LTc}$ and δ^2H_{LTc} among all nine measurements were 3.43 ‰ and 19.75 ‰, respectively.

The $\sigma(\delta_{LTc})$ values among the nine measurements were also shown in Table 2. The average $\sigma(\delta^{18}O_{LTc})$ from the upper leaf, middle leaf, and lower leaf was ± 0.18 ‰, ± 3.27 ‰, and ± 2.32 ‰, respectively. The average $\sigma(\delta^2H_{LTc})$ from the upper leaf, middle leaf, and lower leaf was ± 0.39 ‰, ± 8.33 ‰, and ± 4.08 ‰, respectively. As the standard deviation of δ_{LTc} was greater than $\sigma(\delta_{LTc})$ for both ^{18}O and ^2H, the varability of the leaf level chamber method was greater than $\sigma(\delta_{LTc})$ for each

Table 1
The liner regression results between the ^{18}O isotopic composition of transpired water based on isotopic steady state condition method ($\delta^{18}O_{Tx}$) and the ^{18}O isotopic composition of transpired water based on the chamber method ($\delta^{18}O_{Tc}$), and the liner regression results between the ^{2}H isotopic composition of transpired water based on isotopic steady state condition method ($\delta^{2}H_{Tx}$) and the ^{2}H isotopic composition of transpired water based on the chamber method ($\delta^{2}H_{Tc}$). The slope, intercept, number of regression points (n), coefficient of determination (r^2), correlation coefficient (ρ_r), measure of accuracy (Chen et al.), and concordance correlation coefficient (ρ_c) were selected to evaluate regression. Noted that the regressions in July were not shown due to only two data points remaining after the condensation filter.

Month	Regressions	Slope	Intercept	n	r^2	ρ_r	C_b	ρ_c
May	$\delta^{18}O_{Tx}$ & $\delta^{18}O_{Tc}$	1.00	−0.30	16	0.55^{***}	0.74	0.70	0.52
	$\delta^{2}H_{Tx}$ & $\delta^{2}H_{Tc}$	0.99	−2.11	16	0.63^{***}	0.79	0.77	0.61
June	$\delta^{18}O_{Tx}$ & $\delta^{18}O_{Tc}$	0.96	−0.34	16	0.67^{***}	0.82	0.81	0.66
	$\delta^{2}H_{Tx}$ & $\delta^{2}H_{Tc}$	0.90	−6.60	16	0.85^{***}	0.93	0.92	0.85
August	$\delta^{18}O_{Tx}$ & $\delta^{18}O_{Tc}$	1.04	0.09	9	0.90^{***}	0.95	0.94	0.89
	$\delta^{2}H_{Tx}$ & $\delta^{2}H_{Tc}$	1.07	3.47	9	0.93^{***}	0.96	0.96	0.93
September	$\delta^{18}O_{Tx}$ & $\delta^{18}O_{Tc}$	1.01	−0.25	10	0.59^{**}	0.77	0.71	0.54
	$\delta^{2}H_{Tx}$ & $\delta^{2}H_{Tc}$	1.00	−1.09	10	0.66^{**}	0.82	0.78	0.63
Summarizing	$\delta^{18}O_{Tx}$ & $\delta^{18}O_{Tc}$	0.97	−0.48	54	0.83^{***}	0.91	0.99	0.90
	$\delta^{2}H_{Tx}$ & $\delta^{2}H_{Tc}$	0.99	−0.99	54	0.90^{***}	0.95	1.00	0.94

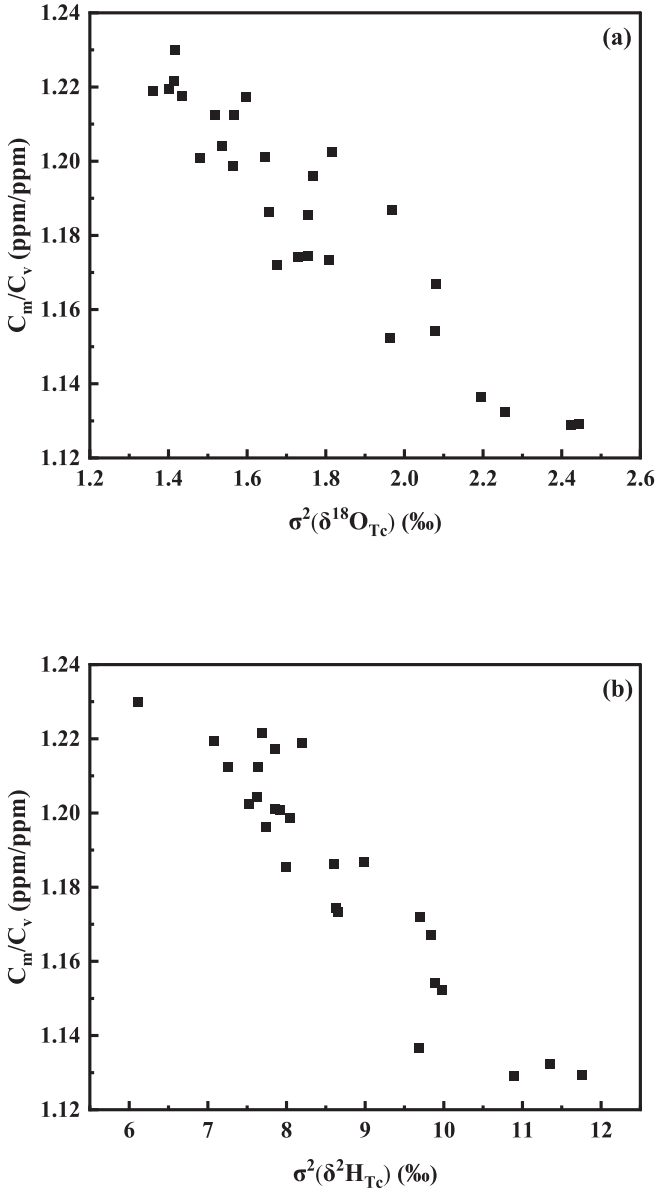

Fig. 3. The relationship between the mixed vapor concentration over background vapor concentration and the square of δ_{Tc} uncertainty in (a) ^{18}O, and (b) ^{2}H.

Table 2
Three leaves from upper, middle, and lower were selected to apply for the chamber method. The chamber method leaf level δ_T ($\delta^{18}O_{LTc}$ and $\delta^{2}H_{LTc}$) and their uncertainties ($\sigma(\delta^{18}O_{LTc})$ and $\sigma(\delta^{2}H_{LTc})$) were listed.

Measurements	Leaf Position	$\delta^{18}O_{LTc}$ (‰)	$\sigma(\delta^{18}O_{LTc})$ (‰)	$\delta^{2}H_{LTc}$ (‰)	$\sigma(\delta^{2}H_{LTc})$ (‰)
1		−5.84	0.19	−51.72	0.43
2	Upper	−5.84	0.16	−51.65	0.39
3		−5.82	0.19	−51.57	0.37
1		−12.96	3.25	−99.52	6.41
2	Middle	−13.02	3.40	−99.81	9.86
3		−12.55	3.17	−98.54	8.73
1		−14.20	2.39	−82.99	3.05
2	Lower	−12.91	2.46	−82.89	4.77
3		−12.63	2.11	−81.98	4.42
Average		−10.64	–	−77.85	–
Standard Deviation		3.43	–	19.75	–

measurment. Thus, applying the chamber method to the whole plant level is necessary to avoid leaf level heterogeneity impacts.

4. Discussion

4.1. The reliability of the chamber method applied in whole corn plant

The ISS method and the chamber method had strong regression significance in both ^{18}O and ^{2}H supporting the validity of both methods. r^2, ρ_r, C_b, and ρ_c had similar trends, indicating precision and accuracy variability of the chamber method were consistent. The uncertainty analysis showed that the highest uncertainty was in May, when the chamber method had the lowest precision ($\rho_r = 0.74$ for ^{18}O, and $\rho_r = 0.79$ for ^{2}H) and accuracy ($C_b = 0.70$ for ^{18}O, and $C_b = 0.77$ for ^{2}H). The lowest uncertainty was revealed in August, when the chamber method had the highest precision ($\rho_r = 0.95$ for ^{18}O, and $\rho_r = 0.96$ for ^{2}H) and accuracy ($C_b = 0.94$ for ^{18}O, and $C_b = 0.96$ for ^{2}H). Thus, the chamber method applied in whole corn plant was more reliable in June and August (summer excluding July) than in May and September. Therefore, the chamber method applied in whole corn plant was reliable during the summertime.

The accuracy, precision, and uncertainty of the chamber method was evaluated with δ_x under steady-state conditions. The most general method to approximate δ_T was using the ISS assumption to cryogenically extract the water from a xylem sample (West et al., 2006), until Chen et al. (2020) found that a cryogenic extraction-associated methodology would bring significant deviations of ^{2}H rather than ^{18}O in δ_T and δ_x, especially in woody plants (Barbeta et al., 2022). Kübert et al. (2023) found less significant deviations between the cryogenic extracted xylem samples and the chamber-based with measured δ_T on *Piper auritum* (herbaceous) than on *Clitoria fairchildiana* (woody). As an herbaceous

plant, maize cryogenic extracted δ_x might therefore have low errors. The strong correlation between δ_{Tc} and δ_x in this study also supported the validity of cryogenic extraction-associated methodology in maize.

Condensation quality control was important for the chamber method. Although the weather conditions were similar in June, July, and August, 85.7 % of the chamber method measurements in July did not pass the quality control due to the condensation of water in the chamber. If the 19 potentially biased values were kept, the linear regressions between δ_{Tx} and δ_{Tc} for ^{18}O would have been less significant ($\delta^{18}O_{Tc} = 0.84\ \delta^{18}O_{Tx} - 1.93$ ‰, $r^2 = 0.80$, n = 72) than for those after applying the condensation quality control filter ($\delta^{18}O_{Tc} = 0.97\ \delta^{18}O_{Tx} - 0.48$ ‰, $r^2 = 0.83$, n = 53). If the quality control filter had not been applied, $\sigma(\delta_{Tc})$ of ^2H could have been ± 8.63 ‰ and $\sigma(\delta_{Tc})$ of ^{18}O could have been ± 1.76 ‰. It was also reported that if a condensation filter was not used before analyzing the data, the chamber method-based δ_T would have larger uncertainty than the chamber method-based δ_E (Han et al., 2022).

4.2. The main factors affecting the chamber method uncertainty

As $\sigma(\delta_m)$ and $\sigma(\delta_v)$ are measured by the same analyzer, we have measurements of $\sigma(\delta_m) = \sigma(\delta_v) = \sigma(\delta)$, where $\sigma(\delta)$ is the uncertainty of vapor isotopic composition measured by our isotope analyzer. In this study, $\sigma(\delta)$ is 0.2 ‰ for ^{18}O and 1.0 for ^2H‰. Similarly, we have $\sigma(C_m) = \sigma(C_v) = \sigma(C)$, where $\sigma(C)$ is the uncertainty of vapor concentration measured by the isotope analyzer. Results in section 3.2 proved that $\sigma(\delta_m) = \sigma(\delta_v)$, and $\sigma(C_m) = \sigma(C_v)$. As $\sigma(\delta)$ is concentration dependent, $\sigma(C)$ can be ignored when calibrating $\sigma(\delta)$(Bailey et al., 2015). Our results also showed that $\sigma(\delta)$ was far greater than $\sigma(C)$ (7.75 times larger for ^{18}O, and 14.53 times larger for ^2H). Therefore, $\sigma(\delta_{Tc})$ could be estimated by $\sigma(\delta)$ and C_m/C_v, and the Eq. (7) could be simplified as:

$$\sigma^2(\delta_{Tc}) \approx \left[\frac{\partial^2(\delta_{Tc})}{\partial^2(\delta_m)} + \frac{\partial^2(\delta_{Tc})}{\partial^2(\delta_v)}\right]\sigma^2(\delta) = \left[1 + \frac{2(C_m/C_v)}{(C_m/C_v - 1)^2}\right]\sigma^2(\delta) = \sigma^2_{est}(\delta_{Tc}) \quad (9)$$

where $\sigma_{est}(\delta_{Tc})$ is the estimated uncertainty of δ_{Tc}. The $\sigma_{est}(\delta_{Tc})$ and $\sigma(\delta_{Tc})$ linear regression was strongly significant for both ^{18}O and ^2H (Fig. 4). As $C_m > C_v$, $\sigma(\delta_{Tc})$ is always greater than $\sigma(\delta)$. This derivation explained an unresolved question as to why the chamber method uncertainty would always be greater than the isotope analyzer system errors (Wang et al., 2012). Allen and Kirchner (2022) showed large propagation of uncertainties when using the isotopic mixing model, which was what the chamber method based on. When C_m is close to C_v (when $\lim_{C_m \to C_v} \frac{C_m}{C_v} = 1$), $\sigma(\delta_{Tc})$ tends to be large. When $C_m \gg C_v$, $\sigma(\delta_{Tc})$ tends to be $\sigma(\delta)$ but always greater than $\sigma(\delta)$. Thus, the value of C_m/C_v mainly affects $\sigma(\delta_{Tc})$. The average C_m/C_v in May was the lowest, corresponding to the greatest average $\sigma(\delta_{Tc})$ in May.

The chamber method has been considered a direct and accurate measurement of δ_T (Wang et al., 2012; Lanning et al., 2020; Kübert et al., 2023). Wang et al. (2012) verified the chamber method in six trials with a known vapor source: With an approximate $C_m/C_v = 1.40$ in the lab, the standard deviations between the δ_{Tc} and the source vapor were 1.00 ‰ for ^{18}O and 1.60 ‰ for ^2H. If inserting $C_m/C_v = 1.40$ into Eq. (9), the expectation of $\sigma_{est}(\delta_{Tc})$ in Wang et al. (2012)'s study would be 0.43 ‰ for ^{18}O and 4.30 ‰ for ^2H, which would be close to the observations here. However, the average C_m/C_v in May, June, July, August, and September in this study was 1.15, 1.20, 1.22, 1.18, and 1.19, respectively. A lower C_m/C_v will bring about larger δ_{Tc} uncertainty, and we cannot determine a constant chamber method precision without considering the chamber conditions.

4.3. Remarks on the chamber method

As C_m is a mix of transpiration-attributed concentration and C_v, increasing plant transpiration would decrease $\sigma(\delta_{Tc})$. Although previous researchers found a similar phenomenon, a mechanistic explanation is still lacking. Dubbert et al. (2014) found the chamber method would have fewer deviations in summer than in spring and autumn when applying in *Quercus suber*. Lu et al. (2017) also found the chamber based δ_T biases would continuously decline from late July to late August with the continuous increase of the leaf area index and ET at a *Sorghum bicolor* field. At a rice field in Japan, it was reported that $\sigma(\delta_{Tc})$ would be larger in May and June with smaller leaf area index and the evapotranspiration compared to that of in July, August, and September (Wei et al., 2015). The largest $\sigma(\delta_{Tc})$ of ^2H in May in Wei et al. (2015)'s study was around 50 ‰, which was 31.25 times the average $\sigma(\delta_{Tc})$ reported in Wang et al. (2012).

The chamber method has also been applied to measuring δ_E. As T occupies most of the terrestrial ET (Jasechko et al., 2013), evaporation-attributed concentration would be relative small to make $C_m \approx C_v$ when obtaining chamber-based δ_E. This might bring about large uncertainty on chamber-based δ_E, which could explain the large off-set between the chamber-based δ_E and the Craig-Gordon-based δ_E (Wang et al., 2013; Wu et al., 2017). Cui et al. (2020) also reported the larger uncertainty of

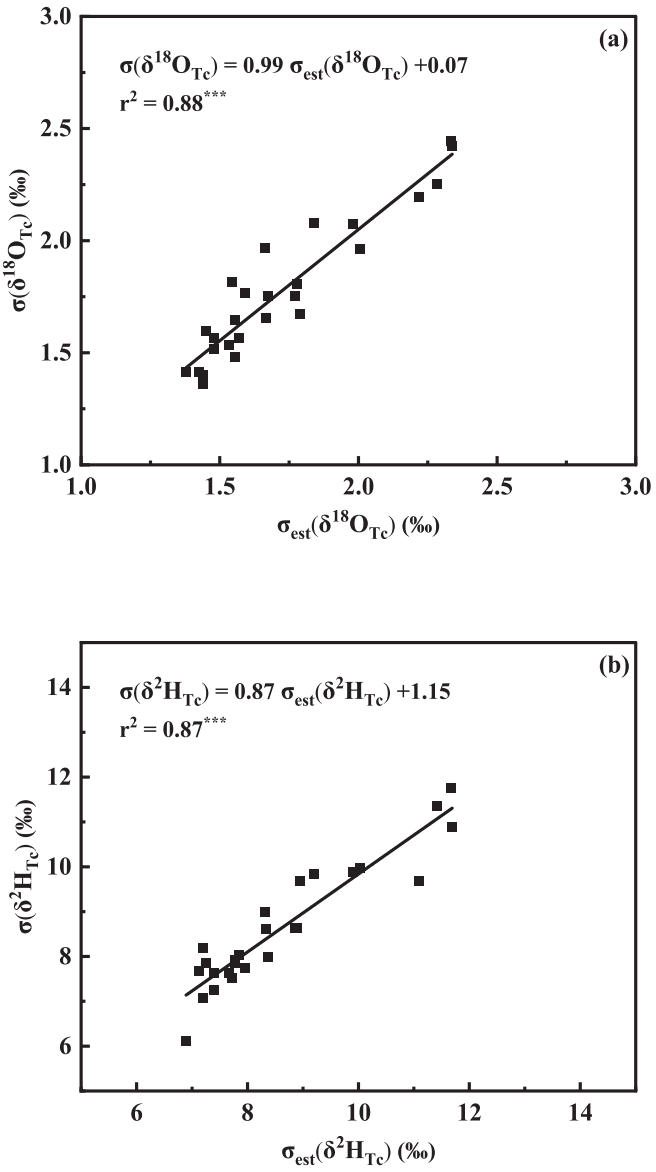

Fig. 4. The relationship between the uncertainty of the chamber method (δ_{Tc}) and the estimated chamber method uncertainty of δ_{Tc} in (a) ^{18}O, and (b) ^2H.

the chamber-based δ_E compared to the chamber-based δ_T on July 15, 2016, at an alpine meadow ecosystem (other dates chamber method uncertainties are not clear). Thus, more careful uncertainty checks should be considered when measuring the chamber-based δ_E.

Previous chamber method evaluations have been focused on the difference between using ^2H and using ^{18}O (Wang et al., 2012), comparing big and small sized chambers (Cui et al., 2020), and using mass balance equation versus the Keeling plots (Wang et al., 2013). In Wang et al. (2012)'s study, $\sigma(\delta_{Tc})$ for ^2H was only 1.60 times of the analyzer's output uncertainty, but $\sigma(\delta_{Tc})$ for ^{18}O was 10.00 times of the analyzer's output uncertainty. In this study, $\sigma(\delta_{Tc})$ for ^2H was 8.45 times of the analyzer's output uncertainty, and $\sigma(\delta_{Tc})$ for ^{18}O was 8.60 times the analyzer's output uncertainty, with no significant difference. Cui et al. (2020) found great consistency between the small and big chambers except when δ_E was relatively small. That might be due to C_m/C_v value being over 2.15 at the alpine meadow ecosystem, where the chamber method's uncertainty was relatively low. Rather than mass-balance-based chamber method intercepting the initial and end step of the vapor mixing, the Keeling plot focuses on the vapor mixing process during the chamber flux measurement. There was a limitation in this study such that other measurements (switch the inlet) between the initial and end step of the vapor mixing, which inhibited monitoring of the mixing process. Although it has been proved that using the mass balance equation versus using the Keeling plot typically provided great consistency (Wang et al., 2013), it would be interesting to test the Keeling-plot-based chamber method uncertainty in future studies.

4.4. Criteria of the chamber method

Previously, the chamber method uncertainty was considered mainly from water vapor condensation within the chamber (Rothfuss et al., 2021). However, the large uncertainty was found during the low transpiration seasons from this study and other studies (Wei et al., 2015; Lu et al., 2017; Wu et al., 2017). The uncertainty analysis has proved that large amounts of transpiration would reduce the chamber method uncertainty. However, too high transpiration would bring about condensation in the chamber. Here, new criteria including three steps to evaluate the chamber method are suggested: 1) Use C_m/C_v values of several test measurements to evaluate whether the chamber method is suitable at the location; 2) The δ_{Tc} data with condensation water should be removed from the analysis regardless of how small the uncertainty; and 3) Present the chamber method uncertainty according to Eq. (7) in this study. Although $\sigma(\delta_{Tc})$ is suggested to be presented in a future study, its threshold depends on the different usage of δ_T. When δ_T is used to estimate T/ET, the uncertainty of δ_T will be mostly transferred to T/ET results when T dominates ET (Chen et al., 2022). In this case, $\sigma(\delta_{Tc})$ should be as small as possible. When δ_T is used for identifying different water sources, $\sigma(\delta_{Tc})$ should be smaller than the difference of each source isotope value to support distinction between the significant differences between each water source.

5. Conclusions

In this study, the ISS method and the chamber method applied for ET measurement on the whole maize plant were compared. The high significance of the regression of the ISS method and the chamber method in both ^{18}O and ^2H are in favor of both methods, and supported the validity of cryogenic extraction-associated methodology in maize stem. The accuracy, precision, and uncertainty of the chamber method were positively correlated. Applying the chamber method to the whole plant level was confirmed to be necessary to avoid the heterogeneity of leaf level chamber method. This study first ever revealed the main factor C_m/C_v that significantly impacts the chamber method uncertainty. A lower C_m/C_v will result in larger δ_{Tc} uncertainty. The chamber method uncertainty would always be greater than the isotope analyzer system errors. The increase of plant transpiration will decrease the chamber method uncertainty. More careful uncertainty checks should be considered when using the chamber method to measure δ_E. A new criterion including three steps was suggested to improve the data quality of the chamber method, which can be used to increase accuracy and decrease uncertainty.

CRediT authorship contribution statement

Yusen Yuan: Writing – review & editing, Writing – original draft, Methodology, Investigation, Funding acquisition, Formal analysis. **Manoj K. Shukla:** Writing – review & editing, Supervision, Conceptualization. **Kenneth C. Carroll:** Writing – review & editing, Supervision, Funding acquisition, Conceptualization. **Lixin Wang:** Writing – review & editing, Methodology, Formal analysis. **Hui Yang:** Methodology, Formal analysis. **Taisheng Du:** Supervision, Funding acquisition, Formal analysis.

Declaration of competing interest

The authors declare that they have no known competing financial interests or personal relationships that could have appeared to influence the work reported in this paper.

Acknowledgements

This work was supported by the Department of Energy Minority Serving Institution Partnership Program (EM MSIPP) managed by the Savannah River National Laboratory under BSRA contract TOA 0000525176, the Research Innovation Fund for Graduate Students of China Agricultural University (2020XYZC39A), and the National Natural Science Foundation of China (52239002, 52109072). We appreciate additional support from the U.S. Department of Energy, Office of Science, Biological and Environmental Research, Biological and Environmental Research - Research and Development Partnership Pilots (DE-SC0023132).

Appendix A. Supplementary data

Supplementary data to this article can be found online at https://doi.org/10.1016/j.jhydrol.2025.133014.

Data availability

Data will be made available on request.

References

Allen, S.T., Kirchner, J.W., 2022. Potential effects of cryogenic extraction biases on plant water source partitioning inferred from xylem-water isotope ratios. Hydrol. Process. 36, e14483.

Bailey, A., Noone, D., Berkelhammer, M., Steen-Larsen, H., Sato, P., 2015. The stability and calibration of water vapor isotope ratio measurements during long-term deployments. Atmos. Meas. Tech. 8, 4521–4538.

Barbeta, A., Burlett, R., Martín-Gómez, P., Fréjaville, B., Devert, N., Wingate, L., Domec, J.c., Ogée, J., 2022. Evidence for distinct isotopic compositions of sap and tissue water in tree stems: consequences for plant water source identification. New Phytol. 233 (3), 1121–1132. https://doi.org/10.1111/nph.17857.

Cernusak, L.A., Barbeta, A., Bush, R.T., Ferrio, J.P., Flanagan, L.B., Gessler, A., Martín-Gómez, P., Hirl, R.T., Kahmen, A., Keitel, C., 2022. Do ^2H and ^{18}O in leaf water reflect environmental drivers differently? New Phytol. 235, 41–51.

Chen, H., Huang, J.J., McBean, E., Dash, S.S., Li, H., Zhang, J., Lan, Z., Gao, J., Zhou, Z., 2022. Evapotranspiration partitioning based on field-stable oxygen isotope observations for an urban locust forest land. Ecohydrology 15, e2431.

Chen, Y., Helliker, B.R., Tang, X., Li, F., Zhou, Y., Song, X., 2020. Stem water cryogenic extraction biases estimation in deuterium isotope composition of plant source water. Proc. Natl. Acad. Sci. 117, 33345–33350.

Craig, H., Gordon, L.I., 1965. Deuterium and oxygen 18 variations in the ocean and the marine atmosphere. E Tongiorgi, Lischi and Figli, Pisa, Italy.

Cui, J., Tian, L., Wei, Z., Huntingford, C., Wang, P., Cai, Z., Ma, N., Wang, L., 2020. Quantifying the controls on evapotranspiration partitioning in the highest alpine meadow ecosystem. Water Resour. Res. 56, e2019WR024815.

Dongmann, G., Nürnberg, H., Förstel, H., Wagener, K., 1974. On the enrichment of $H_2^{18}O$ in the leaves of transpiring plants. Radiat. Environ. Biophys. 11, 41–52.
Dubbert, M., Cuntz, M., Piayda, A., Maguás, C., Werner, C., 2013. Partitioning evapotranspiration–Testing the Craig and Gordon model with field measurements of oxygen isotope ratios of evaporative fluxes. J. Hydrol. 496, 142–153.
Dubbert, M., Cuntz, M., Piayda, A., Werner, C., 2014. Oxygen isotope signatures of transpired water vapor: the role of isotopic non-steady-state transpiration under natural conditions. New Phytol. 203, 1242–1252.
Farquhar, G.D., Cernusak, L.A., 2005. On the isotopic composition of leaf water in the non-steady state. Funct. Plant Biol. 32, 293–303.
Farquhar, G.D., Cernusak, L.A., Barnes, B., 2007. Heavy water fractionation during transpiration. Plant Physiol. 143, 11–18.
Farquhar, G.D., Lloyd, J., 1993. Carbon and oxygen isotope effects in the exchange of carbon dioxide between terrestrial plants and the atmosphere, Stable isotopes and plant carbon-water relations. Elsevier 47–70.
Flanagan, L.B., Comstock, J.P., Ehleringer, J.R., 1991. Comparison of modeled and observed environmental influences on the stable oxygen and hydrogen isotope composition of leaf water in Phaseolus vulgaris L. Plant Physiol. 96, 588–596.
Gan, K.S., Wong, S.C., Yong, J.W.H., Farquhar, G.D., 2002. ^{18}O spatial patterns of vein xylem water, leaf water, and dry matter in cotton leaves. Plant Physiol. 130, 1008–1021.
Han, J., Tian, L., Cai, Z., Ren, W., Liu, W., Li, J., Tai, J., 2022. Season-specific evapotranspiration partitioning using dual water isotopes in a Pinus yunnanensis ecosystem, southwest China. J. Hydrol. 608, 127672.
Harwood, K., Gillon, J., Griffiths, H., Broadmeadow, M., 1998. Diurnal variation of $\Delta^{13}CO_2$, $\Delta C^{18}O^{16}O$ and evaporative site enrichment of $\delta H_2^{18}O$ in Piper aduncum under field conditions in Trinidad. Plant Cell Environ. 21, 269–283.
Jasechko, S., Sharp, Z.D., Gibson, J.J., Birks, S.J., Yi, Y., Fawcett, P.J., 2013. Terrestrial water fluxes dominated by transpiration. Nature 496, 347–350.
Keeling, C.D., 1958. The concentration and isotopic abundances of atmospheric carbon dioxide in rural areas. Geochim. Cosmochim. Acta 13, 322–334.
Kerstel, E., Gianfrani, L., 2008. Advances in laser-based isotope ratio measurements: selected applications. Appl. Phys. B 92, 439–449.
Kübert, A., Dubbert, M., Bamberger, I., Kühnhammer, K., Beyer, M., van Haren, J., Bailey, K., Hu, J., Meredith, L.K., Nemiah Ladd, S., 2023. Tracing plant source water dynamics during drought by continuous transpiration measurements: An in-situ stable isotope approach. Plant Cell Environ. 46, 133–149.
Lai, C.-T., Ometto, J.P., Berry, J.A., Martinelli, L.A., Domingues, T.F., Ehleringer, J.R., 2008. Life form-specific variations in leaf water oxygen-18 enrichment in Amazonian vegetation. Oecologia 157, 197–210.
Lanning, M., Wang, L., Benson, M., Zhang, Q., Novick, K.A., 2020. Canopy isotopic investigation reveals different water uptake dynamics of maples and oaks. Phytochemistry 175, 112389.
Lawrence, I., Lin, K., 1992. Assay validation using the concordance correlation coefficient. Biometrics 599–604.
Lee, X., Kim, K., Smith, R., 2007. Temporal variations of the $^{18}O/^{16}O$ signal of the whole-canopy transpiration in a temperate forest. Global Biogeochem. Cycles 21.
Lu, X., Liang, L.L., Wang, L., Jenerette, G.D., McCabe, M.F., Grantz, D.A., 2017. Partitioning of evapotranspiration using a stable isotope technique in an arid and high temperature agricultural production system. Agric Water Manag 179, 103–109.
Nilsson, M., Alerstam, E., Wirestam, R., Sta, F., Brockstedt, S., Lätt, J., 2010. Evaluating the accuracy and precision of a two-compartment Kärger model using Monte Carlo simulations. J. Magn. Reson. 206, 59–67.
Orlowski, N., Frede, H.-G., Brüggemann, N., Breuer, L., 2013. Validation and application of a cryogenic vacuum extraction system for soil and plant water extraction for isotope analysis. J. Sens. Sens. Syst. 2, 179–193.
Peters, L.I., Yakir, D., 2010. A rapid method for the sampling of atmospheric water vapour for isotopic analysis. Rapid Commun. Mass Spectrom. 24, 103–108.
Phillips, D.L., Gregg, J.W., 2001. Uncertainty in source partitioning using stable isotopes. Oecologia 127, 171–179.
Roden, J.S., Ehleringer, J.R., 1999. Observations of hydrogen and oxygen isotopes in leaf water confirm the Craig-Gordon model under wide-ranging environmental conditions. Plant Physiol. 120, 1165–1174.
Rothfuss, Y., Quade, M., Brüggemann, N., Graf, A., Vereecken, H., Dubbert, M., 2021. Reviews and syntheses: Gaining insights into evapotranspiration partitioning with novel isotopic monitoring methods. Biogeosciences 18, 3701–3732.
Song, X., Simonin, K.A., Loucos, K.E., Barbour, M.M., 2015. Modelling non-steady-state isotope enrichment of leaf water in a gas-exchange cuvette environment. Plant Cell Environ. 38, 2618–2628.
Tetens, O., 1930. Uber einige meteorologische Begriffe. Z. Geophys 6, 297–309.
Tian, F., Hou, M., Qiu, Y., Zhang, T., Yuan, Y., 2020. Salinity stress effects on transpiration and plant growth under different salinity soil levels based on thermal infrared remote (TIR) technique. Geoderma 357, 113961.
Caemmerer, S.v., Farquhar, G.D., 1981. Some relationships between the biochemistry of photosynthesis and the gas exchange of leaves. Planta 153 (4), 376–387. https://doi.org/10.1007/bf00384257.
Wang, K., Dickinson, R.E., 2012. A review of global terrestrial evapotranspiration: Observation, modeling, climatology, and climatic variability. Rev. Geophys. 50.
Wang, L., Caylor, K.K., Dragoni, D., 2009. On the calibration of continuous, high-precision $\delta^{18}O$ and $\delta^{2}H$ measurements using an off-axis integrated cavity output spectrometer. Rapid Communications in Mass Spectrometry: an International Journal Devoted to the Rapid Dissemination of Up-to-the-Minute Research in Mass Spectrometry 23, 530–536.
Wang, L., Good, S.P., Caylor, K.K., 2014. Global synthesis of vegetation control on evapotranspiration partitioning. Geophys. Res. Lett. 41, 6753–6757.
Wang, L., Good, S.P., Caylor, K.K., Cernusak, L.A., 2012. Direct quantification of leaf transpiration isotopic composition. Agric. for. Meteorol. 154, 127–135.
Wang, L., Niu, S., Good, S.P., Soderberg, K., McCabe, M.F., Sherry, R.A., Luo, Y., Zhou, X., Xia, J., Caylor, K.K., 2013. The effect of warming on grassland evapotranspiration partitioning using laser-based isotope monitoring techniques. Geochim. Cosmochim. Acta 111, 28–38.
Wang, P., Yamanaka, T., Li, X.-Y., Wei, Z., 2015. Partitioning evapotranspiration in a temperate grassland ecosystem: Numerical modeling with isotopic tracers. Agric. for. Meteorol. 208, 16–31.
Wang, P., Yamanaka, T., Li, X.-Y., Wu, X., Chen, B., Liu, Y., Wei, Z., Ma, W., 2018. A multiple time scale modeling investigation of leaf water isotope enrichment in a temperate grassland ecosystem. Ecol. Res. 33, 901–915.
Wei, Z., Yoshimura, K., Okazaki, A., Kim, W., Liu, Z., Yokoi, M., 2015. Partitioning of evapotranspiration using high-frequency water vapor isotopic measurement over a rice paddy field. Water Resour. Res. 51, 3716–3729.
Welp, L.R., Lee, X., Kim, K., Griffis, T.J., Billmark, K.A., Baker, J.M., 2008. $\delta^{18}O$ of water vapour, evapotranspiration and the sites of leaf water evaporation in a soybean canopy. Plant Cell Environ. 31, 1214–1228.
West, A.G., Patrickson, S.J., Ehleringer, J.R., 2006. Water extraction times for plant and soil materials used in stable isotope analysis. Rapid Communications in Mass Spectrometry: an International Journal Devoted to the Rapid Dissemination of Up-to-the-Minute Research in Mass Spectrometry 20, 1317–1321.
Wu, Y., 2017. Water Transfer Mechanism and Simulation of SPAC inIrrigated and Film mulch ing Farmland Based on Stable Isotope. China Agricultural University.
Wu, Y., Du, T., Ding, R., Tong, L., Li, S., Wang, L., 2017. Multiple methods to partition evapotranspiration in a maize field. J. Hydrometeorol. 18, 139–149.
Xiao, W., Wei, Z., Wen, X., 2018. Evapotranspiration partitioning at the ecosystem scale using the stable isotope method—A review. Agric. for. Meteorol. 263, 346–361.
Yakir, D., Sternberg, L.d.S.L., 2000. The use of stable isotopes to study ecosystem gas exchange. Oecologia 123, 297–311.
Yuan, Y., Du, T., Wang, H., Wang, L., 2020. Novel Keeling-plot-based methods to estimate the isotopic composition of ambient water vapor. Hydrol. Earth Syst. Sci. 24, 4491–4501.
Yuan, Y., Wang, L., Wang, H., Lin, W., Jiao, W., Du, T., 2022. A modified isotope-based method for potential high-frequency evapotranspiration partitioning. Adv. Water Resour. 160, 104103.
Yuan, Y., Wang, L., Wei, Z., Ajami, H., Wang, H., Du, T., 2024. Using median point in keeling plot to reduce the uncertainty of the isotopic composition of evapotranspiration. J. Hydrometeorol. 25, 637–649.
Zhang, Y., Shen, Y., Sun, H., Gates, J.B., 2011. Evapotranspiration and its partitioning in an irrigated winter wheat field: a combined isotopic and micrometeorologic approach. J. Hydrol. 408, 203–211.
Zhao, L., Liu, X., Wang, N., Kong, Y., Song, Y., He, Z., Liu, Q., Wang, L., 2019. Contribution of recycled moisture to local precipitation in the inland Heihe River Basin. Agric. for. Meteorol. 271, 316–335.
Zhao, L., Wang, L., Cernusak, L.A., Liu, X., Xiao, H., Zhou, M., Zhang, S., 2016. Significant difference in hydrogen isotope composition between xylem and tissue water in Populus euphratica. Plant Cell Environ. 39, 1848–1857.
Zuecco, G., Amin, A., Frentress, J., Engel, M., Marchina, C., Anfodillo, T., Borga, M., Carraro, V., Scandellari, F., Tagliavini, M.J.H., Discussions, E.S.S., 2022. A comparative study of plant water extraction methods for isotopic analyses: scholander-type pressure chamber vs. cryogenic vacuum distillation. Hydrol. Earth Syst. Sci. 26, 3673–3689.